Quantifying nucleosome dynamics and protein binding with PIE-FCCS and spFRET

Martens, C.L.G.

Chapter 4

Nucleosome stability and accessibility depends on linker DNA length, nucleosomal DNA sequence, buffer composition

To facilitate access of proteins like transcription factors to the nucleosomal DNA, nucleosomes spontaneously unwrap DNA from their ends. Transcription factors bind to specific DNA sequences often located at the DNA exits of the nucleosome. To study the effects of the linker DNA and sequence on nucleosome stability and dynamics we constructed sets of mononucleosomes based on the Widom 601 sequence with small variations in these features. We combined Fluorescence Correlation Spectroscopy (FCS) with Pulsed Interleaved Excitation (PIE) and FRET Forster Resonance Energy Transfer (FRET) to quantify DNA unwrapping. Extending the nucleosome with several 10's of base pairs of linker DNA has a stabilizing effect on the nucleosome at low ionic conditions. The effect is reversed at a critical salt concentration inversely proportional to the length of both DNA linkers. A Glucocorticoid Response Element (GRE) in the 601 nucleosome increases the opening and closing rates and affects nucleosomal stability by decreasing electrostatic interactions between DNA and histones, depending on its position with respect to the minor grooves of wrapped DNA. Lastly we show the effect of small changes in buffer composition have on nucleosome dynamics, and discuss irreversible unwrapping occurring on longer timescales. By taking into account these external components and combining PIE-FCS with FRET we quantified the effects of small changes in linker DNA length and nucleosomal DNA sequence on dynamics and stability with increased accuracy and reliability. Hence our technique holds the promise to be suited for probing nucleosomes reconstituted from natural DNA sequences or modified histones, representing the rich but subtle variety of nucleosomes occurring in vivo.

4.1 Introduction

In order to fit inside the nucleus but also be readily available for transcription, DNA needs to be compacted in a non-trivial way. The first level of DNA compaction is the nucleosome, in which the 147 base pairs of DNA are wrapped around an octamer of histones[34][35]. In vivo, nucleosome compaction is modulated by remodelling proteins, transcription factors and other cofactors[96][97][174]. To provide these proteins access to the nucleosomal DNA, nucleosomes spontaneously unwrap DNA from their ends[175][37][51]. This reversible process is called nucleosomal breathing. Forster Resonance Energy Transfer (FRET) has been used to follow nucleosome formation and compaction at nanometer resolution[172][176][53][103][177]. These experiments showed that DNA unwraps at the nucleosomes' exits, yielding access to the nucleosomal DNA. These conformations are referred to as 'open' in contrast to fully wrapped 'closed' nucleosomes. Various in vitro experiments have shown that the interactions between DNA, histones and transcription factors depend strongly on the ionic concentration of the buffer[50][178].
Other single-molecule FRET experiments showed that an increase of linker DNA length in a single nucleosome changed the equilibrium between the open and closed states[104][98][99]. In native chromatin the linker length varies between 10 to 90 base pairs[179][180]. Nucleosomes with longer linker DNA prefer compaction over unwrapping, but the level of compactness is on average lower and has a wider spread[104], indicating increased competition for DNA binding to the histone core. To quantify the role of linker DNA in nucleosome stability and accessibility we designed mononucleosomes with varying linker DNA lengths.
Previous single-molecule studies by Luo et al. have proposed that nucleosomal breathing is the rate-limiting step for specific binding of the LexA protein to its recognition site[100]. For other transcription factors such as the Glucocorticoid Receptor (GR) it has been shown that the position of proteins' recognition sequence in the nucleosome affects binding affinity[39][181][182]. GR is a member of the nuclear receptor family and is translocated to the nucleus upon activation through hormone binding[183][184]. In the nucleus GR interacts directly with DNA, influencing gene expression[185][186][187][188]. According to Wrange et al. the GR prefers binding to a recognition site positioned at a nucleosome exit[94][95] compared to sites closer to the dyad; Jin et

al. showed that the GRs' DNA Binding Domain (DBD) prefers recognition sequences positioned in outward facing minor grooves of the DNA [95]. These and other interaction experiments so far have focused on the binding affinity[94] or bound time[95] of GR to nucleosomes without taking into account the effect of the position of the recognition sequence on nucleosome stability itself. It has been previously shown that nucleosome stability is affected by sequence dependent variations in the nucleosomal DNA[189][190][41][191]. Here we investigate whether the position of a protein recognition sequence has an effect on nucleosome dynamics. Extensive probes have shown transcription factor recognition sites are often located near the nucleosomal DNA exit [192][193][194][195]. To mimic this we have inserted the Glucocorticoid Response Element (GRE) at different positions in a nucleosome and quantified the effect on nucleosome accessibility.
Stabilizing agents like NP-40 are often added to keep nucleosomes from unwrapping in order to study the equilibrium of states[51][50][178][104]. These stabilizers were also added when investigating the affinity of proteins that interact with nucleosomes[100]. Here we will show that addition of NP-40 slows down nucleosome dynamics. Assuming the nucleosome dynamics is the rate-limiting step in protein-nucleosome interactions[50], this means the use of stabilizers in the investigation of these interactions leads to underestimating the affinity.

4.2 Theory

4.2.1 Nucleosome dynamics

Nucleosomal breathing, i.e. switching between an open and closed conformation, is a reversible process governed by the electrostatic interactions between the wrapped DNA and histone tails

$$N_{closed} \underset{k_{closing}}{\overset{k_{opening}}{\rightleftharpoons}} N_{open} \tag{4.1}$$

where N_{open}, N_{closed} represent the open and closed conformations of the nucleosome. The equilibrium between the open and closed states is defined by equilibrium constant

$$K = \frac{[N_{open}]}{[N_{closed}]} \tag{4.2}$$

When nucleosomal DNA unwraps, electrostatic interactions between DNA and histones are broken. After (partially) unwrapping the released DNA attracts m number of cations X^+ from the buffer to replace the positively charged histone residues. Taking these explicitly into account, eq. 4.2 can be rewritten:

$$N_{closed} + m \cdot X^+ \rightleftarrows N_{open} \cdot X_m \tag{4.3}$$

making the equilibrium salt dependent

$$K_X = \frac{[N_{open} \cdot X_m]}{[N_{closed}] \cdot [X^+]^m} = \frac{K}{[X^+]^m} \tag{4.4}$$

Previous experiments on nucleosome breathing indeed showed K to scale exponentially with $[Na^+]$[173]. In order to determine the order of the dependence on the salt concentration from experiments, we rewrite eq. 4.4 such that the number of ions released upon rewrapping of the nucleosomal DNA can be easily extracted from the exponent of the salt dependence of the measured equilibrium between the measured open and closed nucleosomes in the absence of salt[196]:

$$K = K_X \cdot [X^+]^m \tag{4.5}$$

An additional parameter K_0 was added because at low NaCl concentration the equilibrium did not depend on the salt concentration:

$$K = K_X \cdot [X^+]^m + K_0 \tag{4.6}$$

We defined transition concentration c_0 as the concentration where the equilibrium started to be affected by NaCl, i.e. where the first term of eq. 4.6 equals the second term.

4.2.2 Fluorescence Correlation Spectroscopy (FCS)

We used FCS to measure nucleosome dynamics. For this, we used nucleosomal DNA labeled with two fluorescent dyes that form a FRET pair, positioned at the nucleosome dyad and one of the nucleosomal exits. Due to Brownian

motion, the nucleosomes diffuse in and out of the confocal volume, which causes the fluorescence intensity to fluctuate in time[197]. The fluctuations of the intensity were analyzed by correlating the photon arrival times over increasing time-lag τ:

$$G(\tau) = \frac{\langle \delta I(t) \cdot \delta I(t+\tau) \rangle}{\langle I(t) \rangle^2} \tag{4.7}$$

As the fluctuations of fluorescence intensity depend on the concentration and diffusion of the nucleosomes and the confocal volume which they diffuse through, $G(\tau)$ is described by

$$G(\tau) = (V_{eff}C)^{-1} \cdot (1 + \tau/\tau_D)^{-1} \cdot (1 + a^{-2}\tau/\tau_D)^{-1/2} \tag{4.8}$$

with diffusion time τ_D and average number of nucleosomes N in focal volume V_{eff} at concentration C.

4.2.3 Nucleosome dynamics measured with FCS-PIE

The equilibrium between open and closed nucleosomes can also be described kinetically:

$$K_{kin} = \frac{k_{opening}}{k_{closing}} \tag{4.9}$$

As shown by Torres[198] and Tims[199], FCS provides a unique way to obtain these rates. Dividing the autocorrelation curve of the closed nucleosomes as obtained from the nucleosomes that exhibit FRET (G^R_{514}) by the autocorrelation curve of all nucleosomes quantified by the fluorescence of the acceptor dye when excited directly (G^R_{632}) cancels out the diffusion contribution. Instead of performing two separate FCS experiments to obtain these autocorrelation curves[198] or measuring a single sample consecutively with different excitation wavelengths[199], we combine multiple excitation wavelengths through Pulsed Interleaved Excitation (PIE)[137] and use the curves acquired from a single FCS-PIE experiment to prevent effects of different concentrations of nucleosomes between experiments[198] or from decay occurring on longer timescales[199]. The resulting curve mainly represents the nucleosomal dynamics, but also contains a contribution of different photophysical phenomena and detector responses, collectively captured in $G_{photophysics}$:

$$\frac{G^R_{514}}{G^R_{632}}(\tau) = C(\tau) \cdot \left(1 + K_{kin} \cdot e^{-\tau(k_{opening}+k_{closing})}\right) \cdot G_{photophysics} \quad (4.10)$$

Assuming equal diffusion times for open and closed nucleosomes, as done by Torres[198] and Bohm[173] makes the correction factor C(τ) equal to 1. However, previous experiments by Koopmans and Buning on similar nucleosomes as used in this chapter have shown that closed nucleosomes diffuse significantly faster than open nucleosomes[176][53]. Therefore, when calculating G^R_{514}/G^R_{632}, we assumed $\tau_D^{514R} \neq \tau_D^{632R}$ resulting in

$$C(\tau) = \sqrt{\frac{\tau_D^{632R} \cdot (\tau_D^{514R} + \tau)}{\tau_D^{514R} \cdot (\tau_D^{632R} + \tau)}} \quad (4.11)$$

4.3 Materials and methods

4.3.1 Nucleosome reconstitution and sample preparation

DNA containing one Widom 601 sequence and a Cy3B-Atto647N fluorophore pair was produced with PCR. The fluorophores were positioned 80 base pairs apart, thus FRET was possible only when the DNA was reconstituted into a nucleosome. One of two features was added: 1) different lengths of linker DNA or 2) a GR response element (GRE) at the DNA exit of the nucleosome where the fluorophore pair was positioned. Different linker DNA lengths were created by restriction and/or ligation. Nucleosomes were assigned according to their linker lengths with the acceptor dye positioned at the nucleosomal exit near the first linker; e.g nucleosome 39-12 has 39 bp of linker DNA on the Atto647N side and 12 bp of linker DNA on the opposite side. The GRE was inserted through a modified primer at the PCR step (see Supplement for primers and protocols). All nucleosomes were reconstituted by salt gradient dialysis from 2 M to 0 mM NaCl overnight. DNA was mixed with human recombinant histones in a titration of molar ratios ranging from 1:1 to 1:3. Only titrations where no unreconstituted DNA substrates were detected after gel electrophoreris were used for spFRET experiments. Measurement buffers contained 10 mM Tris and 1 mM NaCl, unless stated otherwise. For spFRET burst experiments

nucleosomes were diluted to 80 pM. Nucleosome concentrations in FCS measurements were between 3 and 7 nM. Samples of 20 to 40 μl were placed in a closed flowcell to minimize evaporation. After addition of NaCl, samples were incubated for 2-3 minutes before starting FCS measurements.

4.3.2 Single-molecule fluorescence spectroscopy

Measurements were performed on a home-built confocal microscope with a water-immersion objective (60x, NA 1.2, Olympus), using an ICHROME MLE-SFG laser module (Toptica) as excitation source. The excitation beam was directed via fiber coupler and a dichroic mirror (z514/640rpc, Chroma) through the objective and focused 50 μm above the glass-sample interface. Fluorescence was spatially filtered with a 50 μm pinhole in the image plane and split by a second dichroic mirror (640dcxr, Chroma). The fluorescent signals were further filtered (hq570/100nm and hq700/75nm, for green and red detection resp.) and focused on the active area of single photon avalanche photodiodes (SPADs, SPCM AQR-14, Perkin Elmer). The photodiodes were read out with a TimeHarp 200 photon counting board (Picoquant), and the arrival times were stored in t3r (time-tagged to time-resolved) files. These files were further processed with home-built Python analysis programs based on PyCorrelate[133]. spFRET experiments were done by alternating 514 (60 μW) and 632 nm (60 μW) 25 μs excitation pulses with no intermittent dark periods (alternating laser excitation, i.e. ALEX mode). Data was collected in ALEX-spFRET measurements for 30 to 60 minutes, in which 4000 - 8000 bursts were detected. FCS experiments were performed in pulsed interleaved excitation (PIE) mode by alternating 514 (30 μW) and 632 nm (20 μW) 100 ns excitation pulses with 300 ns intermittent dark periods. PIE-FCS measurements were done for a least 60 minutes, in recordings of 10 minutes.

4.3.3 Burst analysis

The FRET efficiency and stoichiometry were determined from the intensities of photon bursts associated with the donor (I^D) and acceptor (I^A) emission, and FRET signal from the acceptor (I^F). FRET and acceptor bursts were corrected for spectral leakage (α) and direct excitation (δ)[200]. To correct for differences in quantum yield, excitation intensities and detectors (γ),

the FRET efficiency E and stoichiometry S were calculated for each burst as

$$E = \frac{I^F}{I^F + \gamma \cdot I^D} \tag{4.12}$$

and

$$S = \frac{I^F + \gamma \cdot I^D}{I^F + \gamma \cdot I^D + I^A} \tag{4.13}$$

The bursts representing nucleosomes containing both fluorophores ($0.2 < S < 0.8$) were selected and fitted with a double Gaussian. We used the FRETBursts toolkit developed by Ingargiola et al.[133] to calculate E and S and to generate E,S-histograms. We found little variation in the correction factors for all experiments: α: 0.15 $\pm$ 0.03, δ: 0.1 $\pm$ 0.01, and γ: 1.3 $\pm$ 0.1.

4.3.4 Averaged fluorescence intensity analysis

Fluorescence intensity of PIE-FCS measurements of nucleosomes in increasing salt concentrations were first averaged over time (number of photons per second). After corrections for background intensity and spectral leakage the average FRET efficiency was calculated from the average intensities similar to equation 4.10:

$$\langle E \rangle = \frac{\langle I^R_{514} \rangle}{\langle I^R_{514} \rangle + \langle I^G_{514} \rangle} \tag{4.14}$$

and plotted as a function of the NaCl concentration. The result was fitted with the Hill function to investigate the cooperativity of the electrostatic interactions in the nucleosome:

$$\langle E_H \rangle = \langle E_{min} \rangle + \frac{\langle E_{max} \rangle - \langle E_{min} \rangle}{1 + ({}^{[X^+]}/_{c_{1/2}})^{-H}} \tag{4.15}$$

where E_{min} is the bottom asymptote of the average FRET efficiency and E_{max} the top asymptote, $c_{1/2}$ the concentration of NaCl where 50% of the maximal average FRET efficiency is observed The Hill coefficient H indicates the cooperativity of the DNA-histone interactions in the presence of increasing NaCl concentration.

4.3.5 FCS analysis

We used the Python pycorrelate module developed by Ingargiola et al.[133] to calculate all correlation curves. The correlation algorithm used in this module was developed by Laurence et al.[134]. The algorithm is based on rewriting the correlation as a counting operation on photon pairs and can be used with arbitrary bin widths and spacing.
Parameter a (eq. 4.8) is the ratio between the axial and radial dimensions of the confocal volume and was determined through calibration experiments to be 8. Post-fit corrections were done to correct for the effects of background intensity, spectral leakage, the difference of confocal volume for different excitation wavelengths and imperfect volume overlap due to misalignment[138][139] on the number of nucleosomes. From the corrected numbers of open and closed nucleosomes we calculated the equilibrium constant K (eq. 4.2). Kinetic rates $k_{opening}$, $k_{closing}$ were determined by fitting eq. 4.7 to G^R_{514}/G^R_{632}. K_{el}, K_0 and m were found by fitting eq. 4.5 to K. c_0 was calculated by taking the intersect of K_{ind} with $K_{el} \cdot [Na^+]^m$. Error bars in all graphs show the standard deviations from N $>$ 5 measurements.

4.4 Results

4.4.1 Nucleosome conformation at low NaCl concentration

To determine the intrinsic equilibrium constant for nucleosome breathing nucleosome 39-12 was measured in spFRET-ALEX at picomolar concentration. The corrected E, S-histogram in Figure **4.1b** highlights the population of bursts containing both fluorescent labels ($0.2 < S < 0.7$). The FRET distribution of these bursts was fitted with a double Gaussian and revealed a high-FRET population (69%) centered around $E = 0.5 \pm 0.2$ (center $\pm$ width) containing 3202 bursts. The low-FRET population was at $E = 0.04 \pm 0.15$ and contained 1404 bursts. The ratio of the high-FRET and low-FRET bursts yielded $K_{eq} = 0.4$. So, at low ionic concentration, the nucleosome is 70% of the time in the closed conformation.

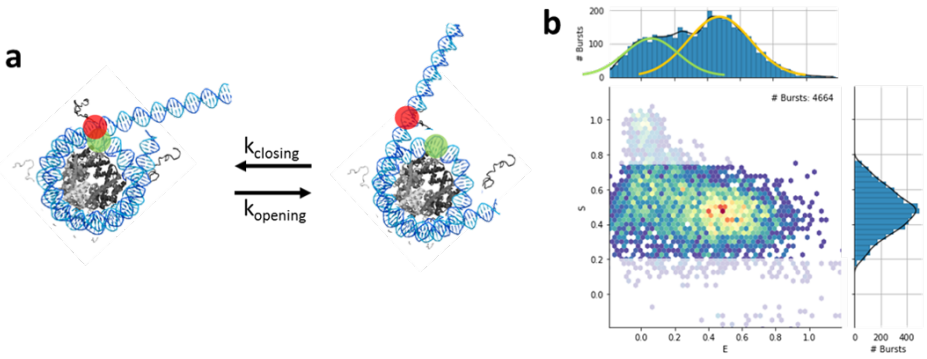

FIGURE 4.1: **Burst analysis of spFRET-ALEX measurement reveals the closed state as the preferred conformation of nucleosome 39-12 at low NaCl concentration. a)** Nucleosomes switch between an open and a closed conformation; when closed, the nucleosome is more compacted and FRET occurs. **b)** The E, S-histogram of a spFRET-ALEX measurement on nucleosomes as depicted in a) shows the majority of the bursts to have a high FRET value (E = 0.48). A double Gaussian fit reveals the low FRET population around E = 0.04. The high FRET population accounted for 3202 bursts and consisted of 69% of all bursts.

4.4.2 Electrostatic interactions in nucleosome 39-12

Nucleosome 39-12 was diluted to nanomolar concentration in 10 mM Tris and NaCl was titrated up to 50 mM. The fluorescence signals of the labels were acquired in PIE-FCS measurements to quantify the concentration and diffusion of the nucleosome and the rates of nucleosome opening and closing.

Figure **4.2a** shows a difference in number of nucleosomes in the closed conformation at 6 mM and 36 mM NaCl. At 6 mM NaCl, the equilibrium constant was approximately 0.5. At 36 mM NaCl, K_{eq} increased to 2. Correlation curves were normalized by the number of nucleosomes detected in the the 632R channel for comparison. The effect of NaCl on the equilibrium is depicted in Figure **4.2b**; the opening rate (bold arrow) increased, while the closing rate (slim arrow) decreased. Cations like Na^+ compete with positive residues on the histones to bind to the negatively charged linker DNA, decreasing nucleosome compaction.

Figure **4.2c** shows a decline of average FRET efficiency <E> at NaCl concentrations between 10 mM and 30 mM NaCl. In that same range the increase cq. decrease in open and closed fractions of nucleosomes seemed to be linear (Figures 4.2d and 4.2e).

K_{eq}, the ratio of the open and closed nucleosome fractions, was fitted with equation **4.6**. This yielded a salt-independent equilibrium K_0 of 0.71, a transition concentration c_0 of 20 mM, and salt stoichiometry m of 3.6 ion pairs (see also table **4.1**).

To produce the data for the panels of Figure **4.3**, equation **4.10** was fitted to G^R_{514}/G^R_{632} of each measured concentration of NaCl. Figure **4.3a** shows a typical G^R_{514}/G^R_{632} curve plus fit at 2 mM NaCl. The larger standard deviations for τ smaller than 0.1 ms were caused by photophysics and afterpulsing, at $\tau >$ 50 ms the timescale exceeded the nucleosome diffusion time, resulting in large errors due to the division of small values. For NaCl concentrations lower than 30 mM, nucleosome 39-12 opened 17 times per second and closed 32 times per second, corresponding to an open time of 31 ms and a closed time of 58 ms. The accompanying equilibrium constant (Figure **4.3d**) K_{eq} = 0.53 was similar to the value we found through spFRET burst analysis (0.43). At [NaCl] = 25 mM, a drop occurred for K_{eq}. This seemed to be caused by a decrease of the closing rate to 10 s^{-1} while the opening rate remained 40 s^{-1}. For higher NaCl concentration we saw opening rates increasing significantly, with closing rates remaining

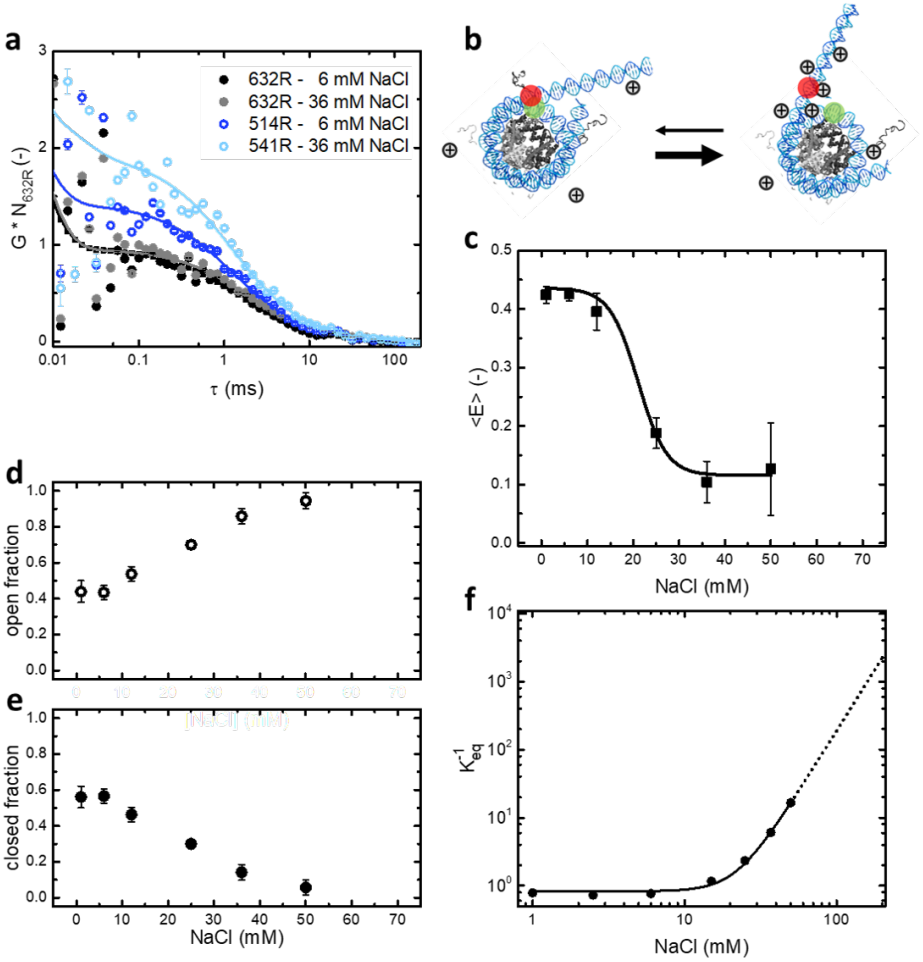

FIGURE 4.2: **Increasing NaCl concentration drives nucleosome 39-12 to the open conformation. a)** Autocorrelation curves of nucleosome 39-12. At 6 mM NaCl the ratio between open and closed states was 1:2. At 36 mM NaCl the ratio was 2:1. **b)** Representation of the ion distribution around the nucleosome. **c)** Increasing [NaCl] lowers the average FRET efficiency non-linearly. Fitting gave $c_{1/2}$ = 21 ± 1 mM and Hill coefficient: 0.14 ± 0.03. **d)** and **e)** Fractions of open and closed nucleosomes increased cq. decreased approximately linearly with the NaCl concentration. **f)** Fitting eq. **4.4** to K_{eq} gave $K_0 = 1.2 \pm 0.07$ and $m = 3.6 \pm 0.1$; c_0 was 20 mM, resembling $c_{1/2}$ of the Hill fit.

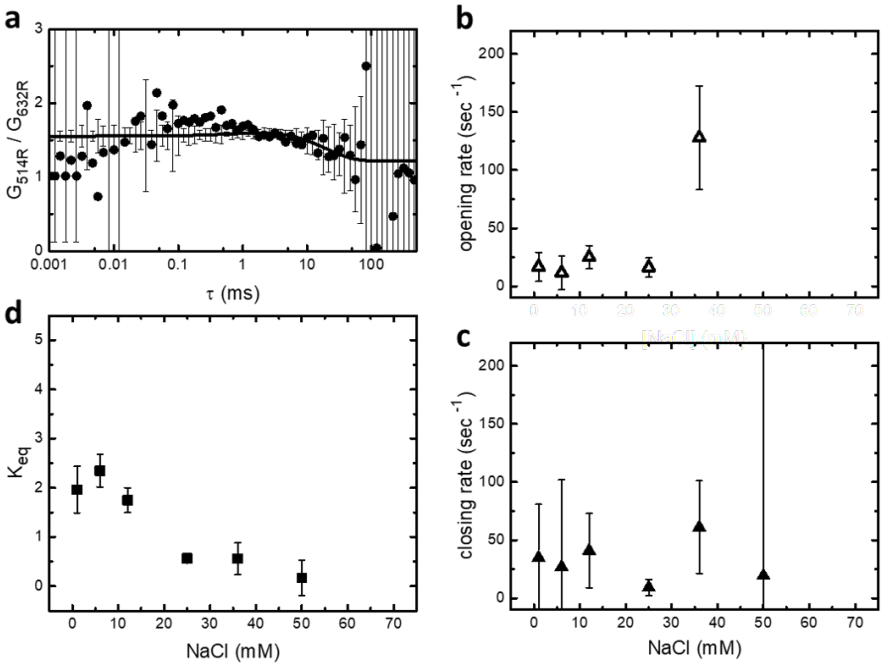

FIGURE 4.3: **Increasing NaCl concentration increased the opening rate; the closing rate remained constant. a)** Dividing ACF 632R by ACF 514R cancels out the diffusional contributions to the curves, the remaining curve represents switching between the open and closed state. **b)** and **c)** Above 30 mM NaCl, the opening rate increased significantly from an average of 17 s^{-1}, to 130 s^{-1}. At 50 mM $k_{opening}$ = 1227 s^{-1} and $k_{closing}$ = 32 s^{-1}. **d)** K_{eq} shows an abrupt drop around 20 mM NaCl, concurring with $c_{1/2}$ = 21 $\pm$ 1 mM.

constant. However, the errors in the fits were relatively large. Nevertheless, the change in K_{eq} at 25 mM NaCl was confirmed by the dynamics analysis, providing credibility to this analysis, despite the relatively large error.

4.4.3 Effects of linker DNA

In chromatin, a nucleosome is flanked by linker DNA of different lengths[179][180]. To test whether the length of the linker DNA has an effect on nucleosomal dynamics we prepared nucleosomes 26-5, 39-100 and 300-12 in addition to nucleosome 39-12. The first number represents the number of base pairs at the exit were the fluorophore pair was positioned, the second number represents the number of base pairs at the opposite exit. The nucleosome dynamics at low salt concentration was first characterized by spFRET burst analysis. Fitting the bursts of nucleosome 26-5 as shown in the E, S-histogram in Figure **4.2a** yielded a high-FRET fraction of 77 % around E = 0.42 $\pm$ 0.2 which contained 2893 bursts (77% of total). The low-FRET fraction was found at E = 0.05 $\pm$ 0.07. Compared to nucleosome 39-12, the fractions of 26-5 were better separated in the E, S-histogram.
The bursts of nucleosome 39-100 appeared more convoluted in Figure **4.4b**. Note that this is the only nucleosome that we tested which had linkers long enough to cross in the closed conformation, bringing the DNA arms in close proximity. Fitting a double Gaussian resulted in a low-FRET population at E = 0.08 $\pm$ 0.14 and a high-FRET population at E = 0.47 $\pm$ 0.2, which consisted of 77% of the 3274 bursts. The E, S-histogram of nucleosome 300-12 displayed two clearly defined populations of bursts (Figure **4.4c**). The high-FRET population consisted of 3551 bursts (65%) with E = 0.44 $\pm$ 0.2. For the low-FRET population we fitted E = -0.03 $\pm$ 0.1.
Nucleosome 300-12 thus had the smallest high-FRET population, followed by 39-12 with 69%. Nucleosomes 26-5 and 39-100 both had 77% of open nucleosomes. Next to characterizing FRET efficiency E and label stoichiometry S, defining the low- and high-FRET populations enabled us to compute the burst widths of these populations. Figure **4.4d** shows that the low-FRET fractions of 26-5 and 39-12 had longer burst widths compared to their high-FRET counterparts. For 39-100 the opposite applies; the low-FRET fraction is 0.5 ms faster than the high-FRET fraction. This suggests that 39-100 nucleosomes were more compacted in a low-FRET conformation. This could be because the 39 base pair linker is unwrapped and the 100 base pair linker wraps towards the histone core. The burst widths of the low- and high-FRET fractions of nucleosome 300-12 are equal. The diffusion of this nucleosome in both open and closed state would be dominated by the 300 base pair DNA linker, which was 10 times larger compared to the diameter of the nucleosome core (100 nm versus 10 nm). The difference in

diffusion times was also visible in the autocorrelation curves of the FRET signal (channel 514R) shown in Figure **4.5a**. The shift to larger τ for longer nucleosomes indicated that diffusion time depends on the length of the linker DNA. The salt dependence of the average FRET efficiency <E> also depended on the linker DNA, but in a different way. Figure **4.5b** shows the FRET efficiency of 39-100 nucleosomes dropped off first, followed by that of 300-12, 39-12 and last 26-5. This means that not only the length of linker DNA, but also the proximity of both linkers (i.e., crossing linker DNA) had a significant effect on nucleosome stability. Fitting the Hill function resulted in $c_{1/2}$'s of 24 $\pm$ 4 mM for 26-5, 21 $\pm$ 1 mM for 39-12, 13 $\pm$ 1 mM for 39-100 and 22 $\pm$ 2 mM (300-12). The Hill coefficient showed negative cooperativity for all nucleosomes: 0.05 $\pm$ 0.02 (26-5), 0.14 $\pm$ 0.03 (39-12), 0.1 $\pm$ 0.02 (39-100) and 0.12 $\pm$ 0.06 (300-12). Thus unwrapping becomes increasingly unlikely as more DNA unwraps. It should be noted that the Hill coefficient heavily depends on the highest and lowest value of <E> for each titration. We observed a difference in average FRET efficiency of the nucleosomes at low salt concentration.

At low NaCl concentration, nucleosomes 26-5, 39-12 and 300-12 all had a closed fraction of $\sim$0.6, despite having different average FRET efficiencies. Nucleosome 39-100 had the highest fraction of closed nucleosomes ($\sim$0.8), an indication that the crossed linker DNA contributed to nucleosome compaction in the absence of cations. The shortest linker DNA had the weakest dependence on NaCl concentration, indicating that electrostatic interactions between the linker DNA and the histones stabilize the nucleosome.

Fitting the number of additional ion pairs m that bind to the nucleosome in the open state quantified this observation. Nucleosome 39-100 had the highest equilibrium constant K_0 (3.8), and 2.3 $\pm$ 0.1 ion pairs bound at the lowest transition concentration c_0 of 13 mM NaCl. There appeared to be a trend for both m and c_0; with increasing linker DNA. The number of bound ions increased from 3.3 $\pm$ 0.1 for 26-5, 3.6 $\pm$ 0.1 for 39-12 to 4 $\pm$ 0.1 for 300-12. The transition concentration decreased from 35 $\pm$ 0.02 mM for 26-5, 22 $\pm$ 0.04 mM for 39-12 to 20 $\pm$ 0.01 mM for 300-12. The increase in bound ions implies that more cations were needed to replace the interactions between histones and DNA when more linker DNA was available in the nucleosome. The decreasing trend for the transition concentration also implies a stronger dependence of nucleosome stability on salt concentration.

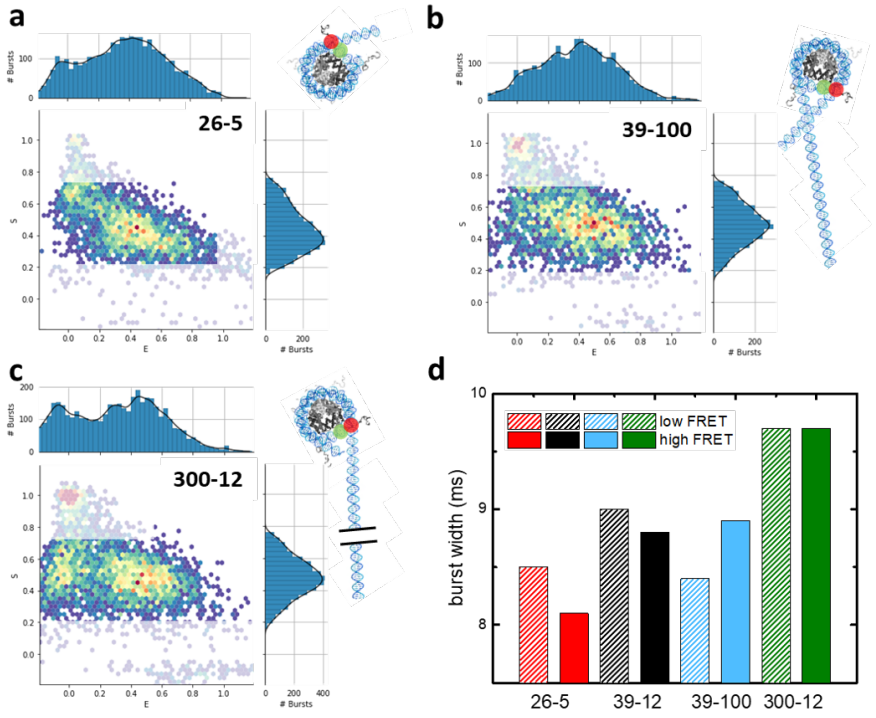

FIGURE 4.4: **Long linker DNA shifts the nucleosome equilibrium to the closed conformation at low NaCl concentration. a)** Nucleosome 26-5 has a larger closed population than nucleosome 39-12; K_{eq} was close to 0.5. **b)** Nucleosome 39-100 featured a small low FRET population and a wider high FRET population,with K_{eq} close to 0.5. **c)** Nucleosome 300-12 yielded $K_{eq} = 0.9$. **d)** The low FRET fractions of 26-5 and 39-12 had a longer burst width caused by a slower diffusion when the nucleosomes are in an open conformation. The burst width of the low FRET population of nucleosome 39-100 was smaller compared to the burst width of the high FRET population. The low and high FRET burst widths for 300-12 are both 9.7 ms.

It can be argued that when histone-linker DNA interactions are disrupted by cations at one position of the linker DNA, the chance for the histone tails to bind to another part of the linker DNA increases. More linker DNA in the nucleosome will then increase the overall chance of histone-DNA interactions taking place at any time, thereby increasing the total energy needed to disrupt these interactions.

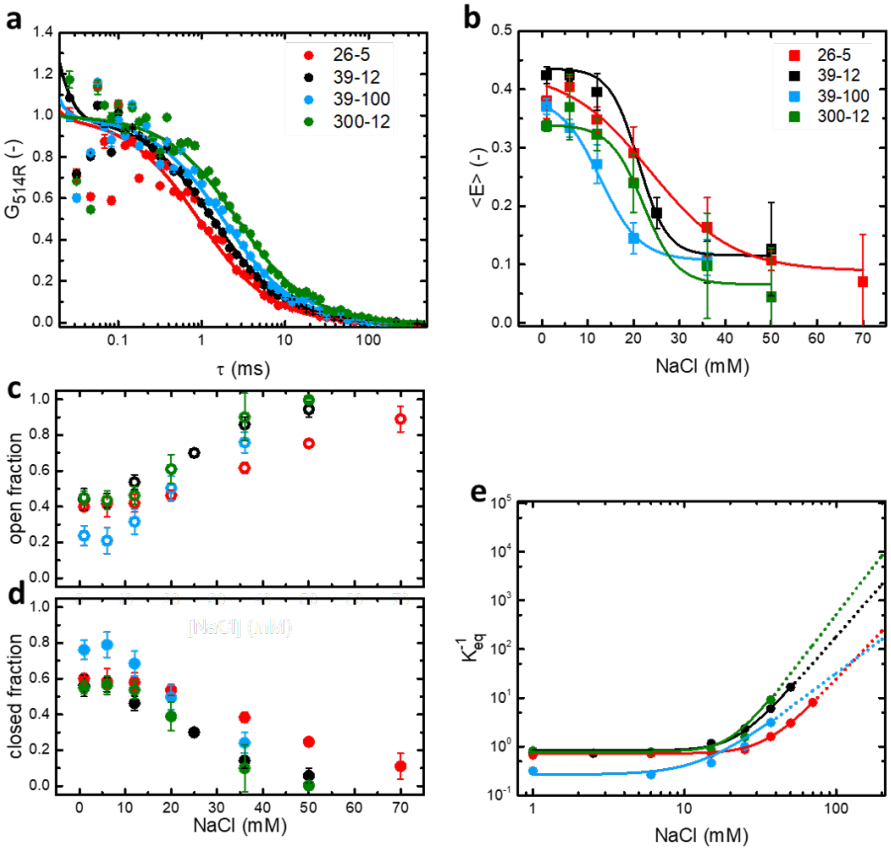

FIGURE 4.5: **Crossing linker DNA increases nucleosome compaction at low NaCl concentration. At increasing NaCl concentration the nucleosome with shorter linker DNA remains compacted longer. a)** The increasing diffusion times of the nucleosomes depend on the length of their linker DNA. **b)** The average FRET shows that at increasing NaCl concentration, nucleosome 26-5 takes the highest NaCl concentration to unwrap, 39-100 the lowest. **c)** and **d)** show for all nucleosomes an approximately linear decrease cq. increase of the closed and open fractions. **e)** Fitting K_{eq} shows that all nucleosomes except 39-100 had a similar K_0; the slopes yielded m = 2.3 for 39-100, 3.3 for 26-5, 3.6 for 39-12 and 4 for 300-12 (see also Table **1**).

When 514R autocorrelation curves were divided by 632R autocorrelation curves the results exhibited large standard deviations for values of τ smaller than 0.1 ms and larger than 50 ms (Figure **4.6a-d**). These large standard deviations should be attributed to spectral characteristics of the fluorophores and the small number of molecules that remain in focus for long times, and were not caused by nucleosome dynamics. Nevertheless, the equilibrium constants calculated from these curves (Figure **4.6e**) showed a trend similar to the decrease of the closed nucleosome fractions (Figure **4.5d**).
At low salt concentration, nucleosome 39-100 had the highest, and nucleosome 300-12 had the lowest value of K_{eq}; increasing NaCl decreased all equilibrium constants, with the K_{eq} of nucleosome 26-5 decreasing slowest. The opening rates of nucleosomes 26-5, 39-12 and 39-100 increased from less than 50 s^{-1} at NaCl concentrations lower than 20 mM to rates of several hundreds per second above this concentration. For nucleosome 300-12 $k_{opening}$ remained stable around 13 ± 7 s^{-1}. The closing rates did not seem to increase with NaCl concentration within the error margins. For NaCl concentrations below 20 mM both nucleosome 26-5 and nucleosome 39-100 had a twice as high $k_{closing}$ compared to nucleosome 39-12 and nucleosome 300-12 (more than 100 s^{-1} versus less than 50 s^{-1}). Higher closing rates (nucleosomes 26-5 and 39-100) were associated with a smaller number of bound ions (m = 3.3 for 26-5 and m = 2.3 for 39-100). The opposite also held; nucleosome 300-12 had the slowest closing and opening rates and a larger number of associated ions (m = 4).

nucleosome	K_X (-)	m (-)	K_0 (-)	c_0 (mM)
$26-5$	$5.4 \pm 1.8 \cdot 10^{-6}$	3.3 ± 0.1	0.71 ± 0.03	34.6 ± 0.02
$39-12$	$1.3 \pm 4.6 \cdot 10^{-6}$	3.6 ± 0.1	0.83 ± 0.07	22.1 ± 0.04
$39-100$	$6.6 \pm 3.3 \cdot 10^{-4}$	2.3 ± 0.1	0.26 ± 0.04	12.8 ± 0.02
$300-12$	$4.3 \pm 1.6 \cdot 10^{-6}$	4.0 ± 0.1	0.77 ± 0.02	20.1 ± 0.01

TABLE 4.1: Crossed linker DNA decreases ionic dependence of nucleosome stability (decrease in m, number of broken ion pairs) short linker DNA shifts equilibrium transition (c_0) to higher NaCl concentration.

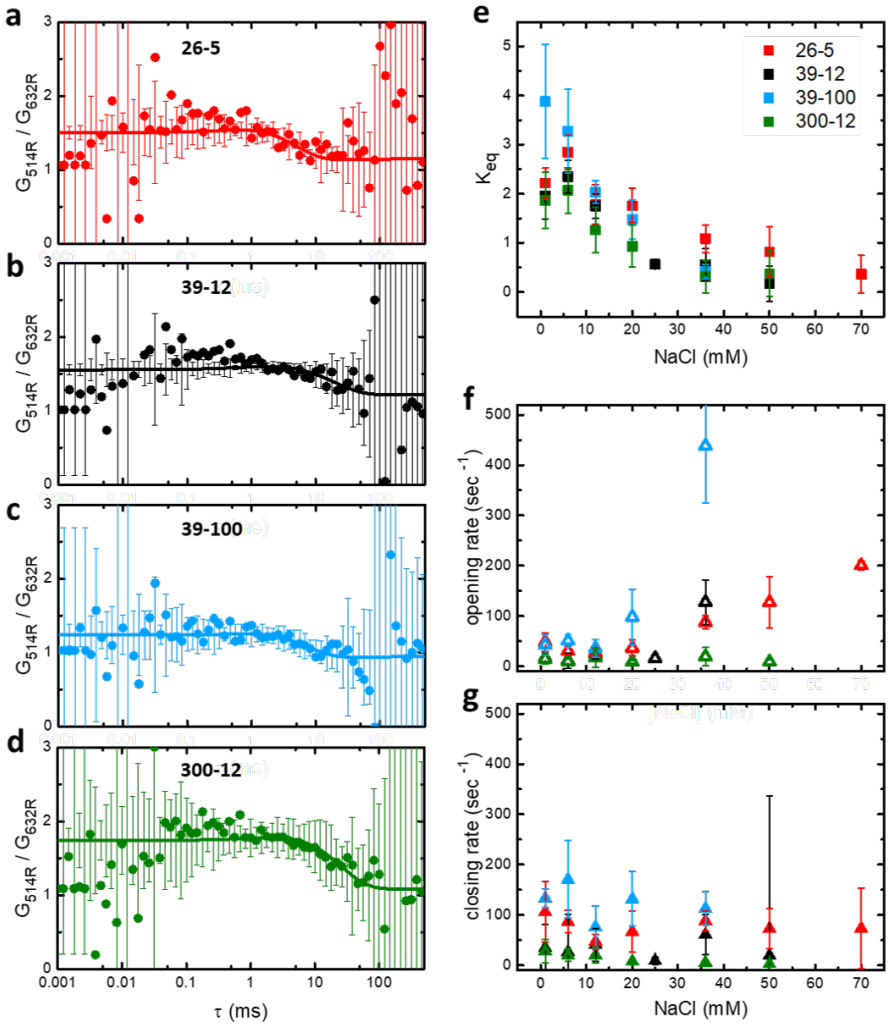

FIGURE 4.6: **Crossed or short linker DNA increased the closing rate at low NaCl concentration, one very long DNA linker decreased both closing and opening rates. a)**, **b)**, **c)** and **d)** are characteristic plots of the dynamics correlation curve for all nucleosomes. **e)** K_{eq} increased for NaCl > 6 mM for all nucleosomes. **f)** Opening rates of nucleosomes 26-5, 39-12 and 39-100 increased at increasing NaCl; $k_{opening}$ of nucleosome 300-12 remained stable. **g)** The closing rates of all nucleosomes did not change significantly upon increasing NaCl concentration.

4.4.4 Effects of nucleosomal DNA sequence

Specific protein recognition sites tend to be enriched at locations in or near DNA exiting from nucleosomes[191][193][194][195]. To resolve the effect of the positioning of such recognition sites relative to the nucleosome, we altered the Widom 601 sequence of nucleosome 39-12 by incorporating a Glucocorticoid Response Element at 3 different positions (GRE1, GRE2 and GRE3).

Figure **4.7a** shows the locations of these sites in the nucleosome. GRE1 was located in two major grooves around SHL -5.5; GRE2 was shifted 5 base pairs into the nucleosome, at two minor grooves (SHLs -5.5 and -4.5); GRE3 was shifted another 5 base pairs, ending up predominantly at two major grooves (SHL -4.5). GRE1 differed 7 base pairs from the 601 template, GRE2 and GRE3 both differed 11 base pairs. We expected GRE2 to show the largest difference with 601 in terms of nucleosome stability and accessibility, since the GRE positioning in the minor grooves is associated with a longer binding time of the GR protein[95]. We anticipated a smaller effect of GRE1. GRE3 was positioned further into the nucleosome which may reduce the effect on nucleosomal breathing dynamics.

However, the only apparent difference in the average FRET efficiency was at high NaCl concentrations (figure **4.7b**) At high salt, GRE1 and GRE2 had lower FRET efficiencies compared to 601 and GRE3. Fitting the Hill function gave similar values for $c_{1/2}$ for all nucleosomes: 21 $\pm$ 1.1 mM (601), 19 $\pm$ 2 mM (GRE1), 21 $\pm$ 0.6 mM (GRE2) and 19 $\pm$ 0.2 mM (GRE3).

The Hill coefficients were also very similar: 0.14 $\pm$ 0.03 (601), 0.1 $\pm$ 0.13 (GRE1), 0.1 $\pm$ 0.01 (GRE2) and 0.15 $\pm$ 0.006 (GRE3), and showed negative cooperativity. All nucleosomes showed a similar decrease in their fractions of closed nucleosomes. Fitting K_{eq} revealed that nucleosomes 601 and GRE1 had the highest number of bound ions with m = 3.6 $\pm$ 0.1 (601) and m = 3.7 $\pm$ 0.1 (GRE1). GRE2 bound ions less strongly (m = 2.7 $\pm$ 0.04) and GRE3 featured the smallest m: 2.0 $\pm$ 0.2. The trend appeared to be that the closer a mutation was located towards the dyad of the nucleosome, the larger its effect on nucleosomal stability.

The transition concentrations showed that nucleosomes 601 and GRE1 were the most stable (c_0 at 22 $\pm$ 0.04 mM and 23 $\pm$ 0.06 mM) GRE3 less (18 $\pm$ 0.12 mM), and GRE2 the least stable (14 $\pm$ 0.03 mM). This implied that nucleosome GRE2 should have higher opening and/or smaller closing rates, compared to nucleosome 601. Because nucleosome GRE1 had similar values

of c_0 and m, and we expected it would have similar dynamics as 601.
The ratio of the autocorrelation curves 514R and 632R at 1 mM NaCl, shown in Figures **4.8a-d**, did not reveal large differences between the nucleosomes. Figure **4.8e** shows that at NaCl concentrations smaller than 20 mM, nucleosomes 601 and GRE1 had slightly higher equilibrium constants than nucleosomes GRE2 and GRE3, implying the first to be closed more often or for a longer period of time.
The transition rates confirmed this: Figure **4.8f** showed that the opening rates of nucleosomes 601, GRE1 and GRE3 increased with increasing NaCl concentration. Like nucleosome 601, GRE3 had an opening rate of around 30 s^{-1} below 25 mM NaCl, but increased less steep as salt increased compared to nucleosome 601. The opening rates of nucleosome GRE1 seemed to increase linearly from $\sim$25 s^{-1} (1 mM NaCl) to $\sim$120 s^{-1} above 20 mM NaCl. The opening rates of nucleosome GRE2 were larger and decreased only marginally from 79 $\pm$ 9 s^{-1}. The steep decrease of the closing rate of nucleosome GRE2 was most obvious from Figure **4.8g**; from faster than 150 s^{-1} at 1 mM NaCl to slower than 50 s^{-1} above 20 mM NaCl. Nucleosome GRE3 appeared to have similar closing rates as nucleosome 601 of $\sim$40 s^{-1}, nucleosome GRE1 was closing more frequently at 60 s^{-1}. The higher opening and closing rates of nucleosome GRE1 could be related to the slightly lower average FRET efficiency shown in Figure **4.7b**; when a nucleosome opened and closed more often, it may not wrap back completely to the histone core, leaving a larger distance between the FRET pair.The number of altered base pairs did not seem to have an effect on nucleosome breathing; the location of the mutation caused the largest differences in nucleosomal stability.

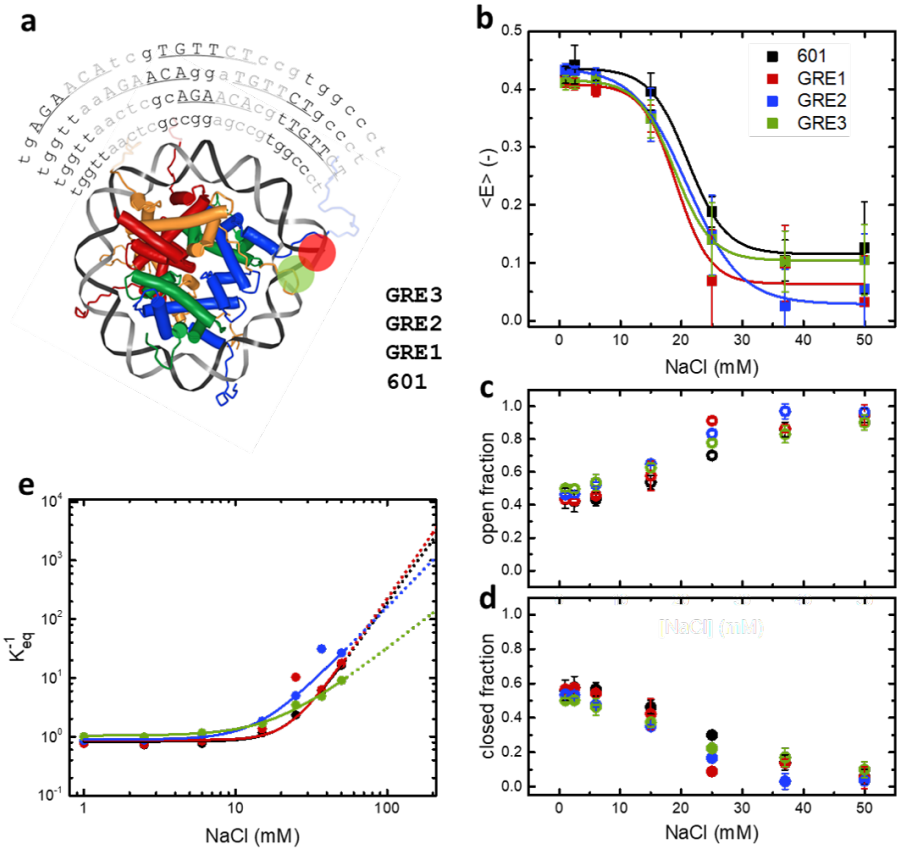

FIGURE 4.7: **DNA sequence has a small effect on nucleosome breathing. a)** Glucocorticoid Response Elements GRE1 and GRE3 were located in major grooves (colored dark grey), GRE2 was introduced in two minor grooves (colored light grey). **b)** The FRET efficiency as a function of salt concentration did not reveal significant differences between all constructs. **c)** and **d)** All nucleosomes had a similar salt dependence for closed and open fractions. **e)** Fitting K_{eq} did reveal small effects of the GRE mutations: m decreased from 601 to GRE3. Concentration c_0 showed that nucleosomes 601 and GRE1 were most stable.

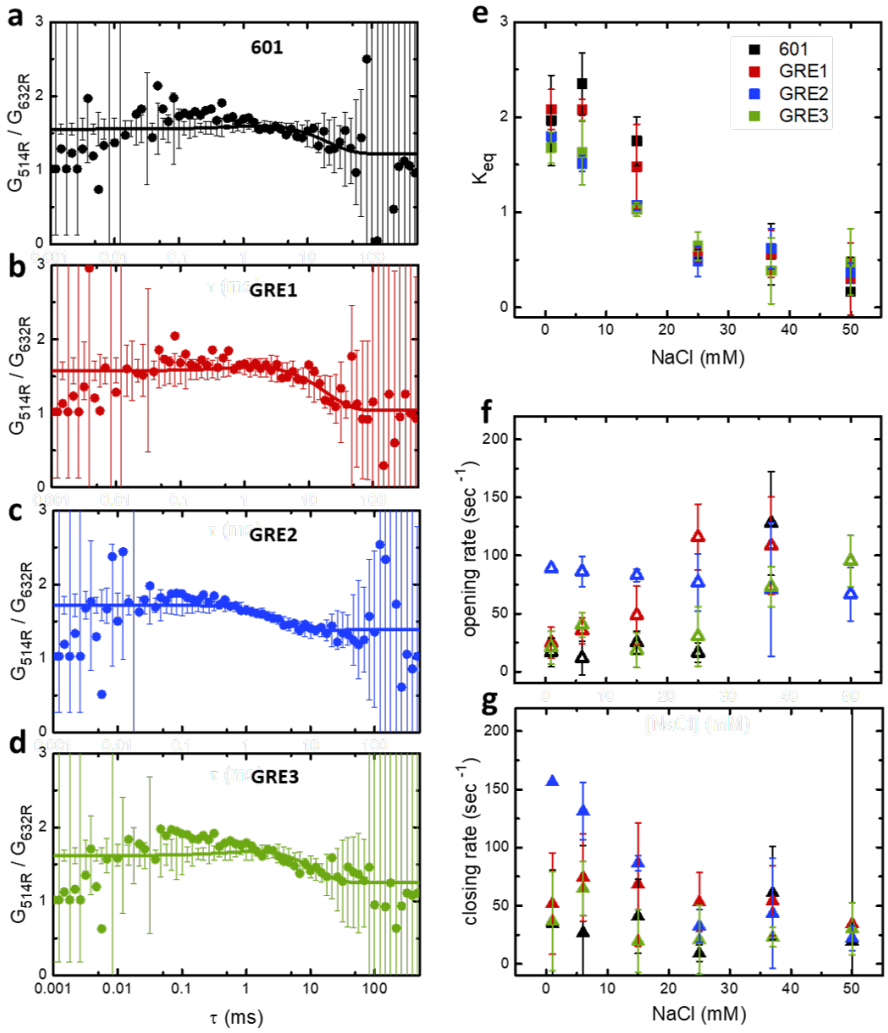

FIGURE 4.8: **Mutation in the minor grooves and close to the exit changed nucleosome dynamics most. a)**, **b)**, **c)** and **d)** show the ratio of 514R and 632R autocorrelation curves for different nucleosomes. **e)** K_{eq} from fitting the relative correlation curves decreased for increasing [NaCl]. **f)** and **g)** Nucleosome GRE2 showed significantly different salt-dependent dynamics.

nucleosome	K_X(-)	m(-)	K_0(-)	c_0(mM)
601	$1.3 \pm 4.6 \cdot 10^{-6}$	3.6 ± 0.1	0.83 ± 0.07	22.1 ± 0.04
GRE1	$6.9 \pm 3.7 \cdot 10^{-6}$	3.7 ± 0.1	0.87 ± 0.11	22.8 ± 0.06
GRE2	$7.6 \pm 1.1 \cdot 10^{-4}$	2.7 ± 0.04	0.89 ± 0.05	14.2 ± 0.03
GRE3	$3 \pm 7 \cdot 10^{-3}$	2.0 ± 0.2	1.04 ± 0.21	18.2 ± 0.12

TABLE 4.2: The most inward mutation (GRE3) has the biggest effect on the nucleosomes' stability, a mutation in the minor grooves (GRE2) affects the equilibrium transition most.

4.4.5 Effects of buffer composition

When studying nucleosomes, other factors that stabilize the nucleosome are often added to the buffer to increase stability[176] or decrease surface interactions[53]. The effect of the additive itself on stability and dynamics is however rarely mentioned. There is no consensus on a standard buffer composition for nucleosome dynamics studies, which makes comparing experiments non-trivial. Here we have studied the effect of tris(hydroxymethyl)aminomethane (Tris) and nonionic detergent octylphenoxypolyethoxyethanol (known as Igepal-CA 630) which are added to increase nucleosome stability. We also tested the effect of Vitamin C, which enhances photostability through reduction of blinking of the fluorophores. However, we did not find a significant difference in photon signals when Vitamin C was added. Figure **4.9a** shows the addition of 0.02% NP40 (and 1mM Vitamin C) reduced the diffusion time of a 39-12 nucleosome almost twofold; it decreased opening and closing rates 3-4 times, and increased the equilibrium constant from 0.47 to 0.29 (see also Table **3**). Increasing the Tris concentration showed a slower decrease of the FRET efficiency than increasing [NaCl] (Figure **4.9d**). FRET remained stable for Tris concentrations below 20 mM and decreased in a linear fashion for higher concentrations. Fitting the observed equilibrium constant yielded an equilibrium K_0 similar to the one found in NaCl titration: 0.9 $\pm$ 0.15 (Tris) and 0.83 $\pm$ 0.07 (NaCl). For Tris the value of m was 7.55 $\pm$ 0.55, suggesting the effective charge of Tris to be half that of monovalent Na. The transition concentration c_0 was also higher at 29 $\pm$ 0.1 mM Tris (22 $\pm$ 0.04 mM for NaCl), implying less effective interactions with the nucleosome.

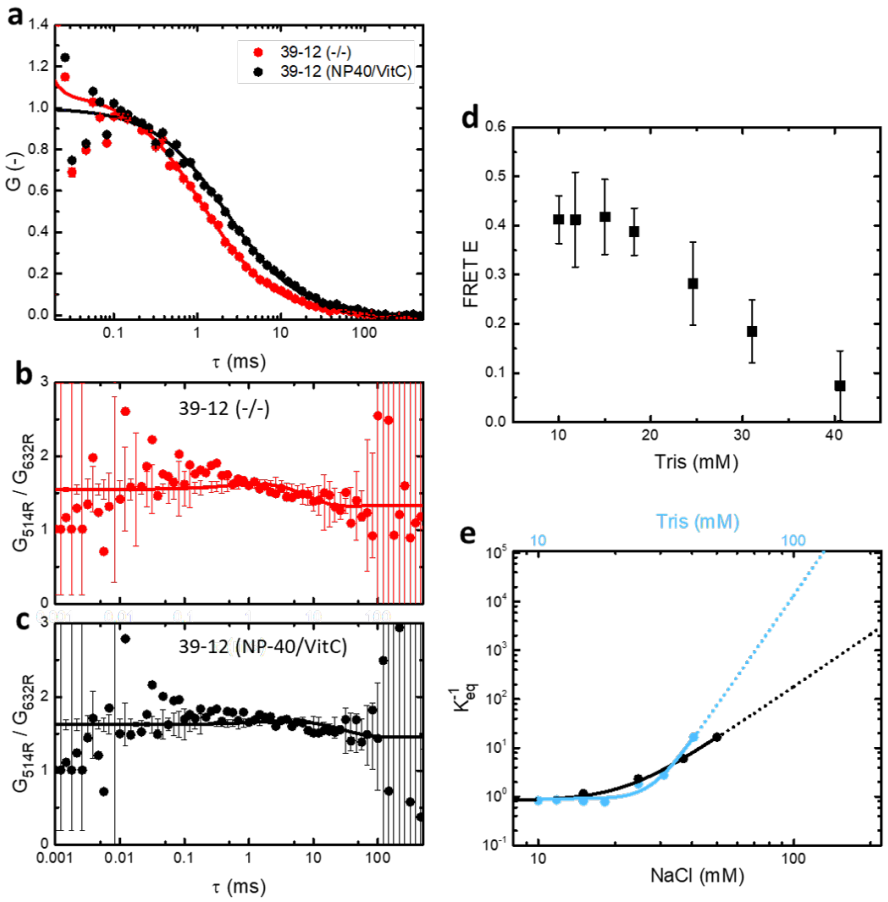

FIGURE 4.9: **Buffer additives have a substantial impact on both stability and dynamics of the nucleosome. a)** Addition of 0.02% NP40 and 1mM Vitamin C slowed the average diffusion time of a nucleosome almost twofold. **b)** and **c)** Characteristic plots of the ratio of the 514R and 632R autocorrelation curves of 39-12 without (b) and with (c) NP40 and Vitamin C. **d)** Adding Tris decreased the FRET efficiency in a similar fashion as seen before with NaCl. **e)** Fitting K of the Tris titration showed an independent equilibrium K_X at a higher transition concentration x_0.

buffer	τ_D (ms)	t_{open}(ms)	t_{close}(ms)	K_{eq}
(-/-) (ms)	1.32 ± 0.25	10 ± 12.5	21 ± 46	2.15 ± 0.47
(NP40/VitC)	2.31 ± 0.35	35 ± 19	121 ± 11	3.46 ± 0.8

TABLE 4.3: Addition of NP40 and Vitamin C decreases diffusion time as well as dynamics of the nucleosome, thereby increasing stability (K_{eq}).

4.5 Discussion and conclusions

In this chapter we quantified the dependence of nucleosomal dynamics and stability on small differences in linker DNA length or DNA sequence by combining PIE-FCS with FRET. In salt concentrations lower than physiological conditions nucleosomes preferred to be in a closed conformation. Upon increasing NaCl concentration the opening rate increased while the closing rate remained the same. DNA-histone interactions strengthened with the length of linker DNA. Surprisingly, the extension of linker DNA lowered the NaCl concentration at which the opening rates of the nucleosome started to increase.
The insertion of the Glucocorticoid Response Element (GRE) in the Widom 601 DNA sequence decreased the stability of the nucleosome when the GRE was inserted deeper into the nucleosome (i.e. towards the dyad). Except for the nucleosome with the GRE in the minor grooves, all GRE nucleosomes increased their opening rates upon increasing NaCl concentration. Positioning the GRE in the minor grooves, where it approached the histone core closer than in the major grooves, did not increase the opening rate but rather decreased the closing rates. The GRE in the minor grooves might increase the rigidity of the DNA strand, making it energetically less favourable to bend towards the histone core. Overall, positioning the GRE towards the dyad decreased the critical NaCl concentration at which equilibrium changed.
The combination of PIE-FCS with FRET allowed to differentiate between open and closed nucleosomes, yielding the equilibrium constant as well as the dynamic rates without extensive corrections. To extract the opening and closing rates from autocorrelation curves, the correlation curve generated from the FRET signal was divided with the curve from the directly excited acceptor, thereby cancelling contributions from diffusion. This method seems to be more robust than dividing correlation curves obtained from

different measurements as reported by Torres et al[198]. Though the error margins were very large at short and long lag times, the equilibrium constant that was derived from fitting the ratios of the correlation curves agreed well with the equilibrium constant derived from the ratio of the fractions of open and closed nucleosomes, validating this method.
Comparing PIE-FCS results with findings from burst analysis for nucleosomes with variable linker DNA lengths in low NaCl concentration added more insight in the effect of linker DNA on compaction. For the nucleosome with crossed linkers, burst analysis did not show a low-FRET population. PIE-FCS data confirmed that this nucleosome was almost completely closed at low ionic conditions. For constructs with crossing linker DNA burst analysis revealed a small low-FRET population, accounting for a higher fraction of open nucleosomes, again consistent with the PIE-FCS data. Quantifying the low- and high-FRET populations did not completely reflect these observations. The nucleosome with the shortest linkers had a high-FRET population comparable to the nucleosome with the crossing linkers in burst analysis, while PIE-FCS showed a closed fraction comparable to nucleosomes without crossing DNA. We argue that this discrepancy originates from the thresholds chosen in burst analysis. Setting parameters such as number of photons and intermittent photon times too narrow results in missing bursts, while setting them too wide results in overestimating the number of bursts. Also, burst analysis can only be properly performed at concentrations < 200 pM to prevent bursts overlapping. When the concentration is too low (< 10 pM) however, it becomes difficult to acquire enough statistics. Moreover, at such low concentrations one has to take into account the reduced nucleosome stability. FCS generates reliable results over several orders of magnitude of concentration (1 pM to 50 nM). Measuring at nanomolar rather than pM concentrations increases the signal to noise ratio, making it less likely to misinterpret FRET signals.
Stabilizer compounds and oxygen scavengers are common ingredients in buffers used for single-molecule experiments on nucleosomes[178][97][176]. These additives reduce the deteriorating effects of low nucleosome concentrations by stabilizing nucleosomes or enhancing emission from fluorophores. We showed however, that nucleosomal dynamics is slowed down significantly and nucleosomes are more in a closed conformation when adding NP-40 and Vitamin C. Indeed, the nucleosome breathing studied here may be the first step in dissociation

of the nucleosome. Even though we did not measure nucleosome stability as a function of increasing salt concentration in the presence of these additives, we expect that the decrease in dynamics and the shift to the closed conformation would still occur at higher salt conditions. One could argue that adding stabilizing agents better resembles the *in vivo* situation, but we want to stress that the effect of additives on dynamics and stability should be taken into consideration when comparing experiments.
In this chapter we report a relatively small range of salt concentrations, up to 70 mM, compared to work previously done by e.g. Gansen[178] and Bohm[173]. There are several reasons for our concentration cap. To quantify the changes in nucleosomal dynamics induced by small sequence and linker length changes at the nucleosomes' exit, the FRET pair was positioned at the dyad and one of the last base pairs in the nucleosome. In concurrence with previous observations, nucleosomes unwrap progressively from the exits towards the dyad[177][99]. When measuring in higher salt conditions (> 100 mM NaCl) we observed that the FRET signal was lost progressively and irreversibly and we could not follow dynamics anymore. A loss of FRET signal was also observed to a lesser degree for salt concentrations lower than 100 mM. We observed that a small fraction of the nucleosomes irreversibly unwrapped over 10-30 minutes, until an equilibrium was reached. Similar progressive unwrapping of nucleosomes has been observed by others[53][201][202] and it was suggested this form of unwrapping resulted in sub-nucleosomal particles such as hexasomes and tetrasomes, which is enhanced by diluting the nucleosomes to low (< 1 nM) concentrations. Because the positions of our FRET pair can not discriminate between open nucleosomes and partially dissociated nucleosomes, we cannot confirm this interpretation. In our measurements however, long-term progressive unwrapping did not depend on nucleosome concentration (measurements were repeated at different nucleosomes concentrations (1 - 20 nM) and same NaCl concentration). Bohm et al.[173] reported before that nucleosomes need to equilibrate for several minutes after changing salt concentration. Taking into consideration that histone-DNA binding energies cannot be determined when dissociation is irreversible[36], we did not include measurements taken immediately after adding salt. Overall, we obtained very similar results from FRET burst analysis and FCS-PIE. The latter allows for a more detailed spectral and temporal analysis though.
We used this method to distinguish structurally highly similar nucleosomes.

We have shown that nucleosomes wrap their DNA more stably when more linker DNA is available, suggesting that the histone tails span out further over the linker DNA. Small changes in nucleosomal DNA sequence affect both nucleosome dynamics and stability. By combining PIE-FCS with FRET we increased robustness and accuracy of measured dynamics and conformation. Hence we are confident that our technique is also applicable on nucleosomes containing natural DNA sequences, which exhibit an even richer variety than the nucleosomes containing the Widom601 sequence used in our experiments. This finding should be taken into account when comparing the binding of transcription factors to their target sites[174][100].